# Thermal Conductivity of Alkali Halide Crystals Containing the Hydroxide Ion*

RALPH L. ROSENBAUM,† CHEUK-KIN CHAU,‡ AND MILES V. KLEIN
*Department of Physics and Materials Research Laboratory, University of Illinois, Urbana, Illinois 61801*
(Received 28 March 1969)

Thermal-conductivity measurements have been performed from 0.34 to 80°K for alkali halide crystals containing the hydroxide ion as an impurity. For sodium chloride containing hydroxide, bowl-shaped thermal-conductivity curves are measured between 0.4 and 0.9°K; the form of these curves is believed to arise from more than one tunneling energy level of hydroxide in the 0.9- to 2.8-$cm^{-1}$ region. Thermal-conductivity measurements on potassium chloride containing hydroxide suggest the existence of tunneling levels immediately below 0.3°K. Similar measurements on rubidium chloride and potassium iodide with hydroxide suggest the existence of tunneling levels considerably below 0.3°K, with the scattering stronger in the latter system. The tunneling levels of sodium-chloride–sodium-hydroxide show no isotopic dependence when deuteroxide $OD^-$ is substituted for hydroxide $OH^-$. Measurements on lightly doped hydroxide samples were complicated by the presence of significant amounts of divalent calcium impurity that destroys the excited energy levels of hydroxide. The thermal-conductivity data in KCl and NaCl have been fitted quantitatively by computer computations using the Debye thermal-conductivity integral. Resonance phonon scattering rates were used which incorporate temperature-dependent widths as essentially the only adjustable parameters, plus frequency-dependent imaginary parts in the resonance denominators. In some cases the widths determined this way are in good agreement with other data on the linewidths.

## I. INTRODUCTION

THE introduction of a molecular impurity into an alkali halide lattice often gives rise to a tunneling motion of the impurity among regions of the barrier-potential minima. The barrier potential arises from interactions of the lattice with the molecule. A large barrier hinders the rotational motion of a free diatomic molecule and replaces the rotational motion with two new types of motion—the tunneling motion and a two-dimensional harmonic-oscillator motion known as librational motion. The energy levels of the impurity arising from the tunneling, hence known as tunneling levels, fall in the very-far-infrared and short-microwave spectral range. It is known that many of the tunneling levels in solids are strongly coupled to the phonon field in that the phonons are scattered (a change of momentum direction and/or magnitude occurs) through the virtual excitation of the molecular impurity into a higher tunneling energy level. Thus it is possible to probe the tunneling levels with low-temperature thermal-conductivity measurements and also directly with very-far-infrared measurements. This paper deals specifically with experimental thermal-conductivity measurements on some alkali halide crystals doped with the hydroxide impurity $OH^-$ and with computer computations of the thermal conductivity using the Debye thermal-conductivity integral with resonance phonon relaxation rates that incorporate temperature-dependent half-widths.

* Work supported in part by the Advanced Research Projects Agency under Contract No. SD-131.

† Present address: Department of Physics, Technion, Haifa, Israel.

‡ Present address: Department of Physics, Illinois Institute of Technology, Chicago, Ill. 60616.

[1] R. L. Rosenbaum, Ph.D. thesis, University of Illinois, 1968 (unpublished).

## II. MEASUREMENTS

### A. Thermal-Conductivity Data of NaCl:NaOH

The thermal-conductivity measurements were taken in a conventional circulating $He^3$ refrigerator. Primary thermometry of a CMN salt was transferred to a pair of germanium thermometers which measured the temperature gradient and mean temperature of the crystal. Details are found elsewhere.[1] The techniques of crystal growth and characterization have been published previously.[2]

The thermal-conductivity data for NaCl:NaOH are shown in Fig. 1. These curves represent an extension of some earlier results[3,4] to lower temperatures and a wider concentration range. For the pure NaCl curve, the thermal conductivity has a maximum of 9 W/cm °K and decreases on both sides of the maximum. The low-temperature side exhibits a $T^{2.81}$ dependence rather than the expected $T^3$ dependence. This weaker temperature dependence is attributed to incomplete diffuse reflection of the phonons at the crystal surface. It is believed that all the crystals have the same boundary scattering mechanism as the pure crystal, since all crystals have very similar preparation histories.

If we proceed to the data on crystals doped with the hydroxide ion, we notice some general features: (1) The thermal conductivities are strongly depressed in comparison to the pure curve at 4°K and below, (2) the more heavily doped curves exhibit a bowl-shaped form or dip below 1°K, and (3) for the lightly doped crystals, there are discontinuous upward breaks between the data in the $He^3$ and $He^4$ regions.

[2] M. V. Klein, S. O. Kennedy, Tan Ik Gie, and B. Wedding, Mater. Res. Bull. **3**, 677 (1968).

[3] M. V. Klein, Phys. Rev. **122**, 393 (1961); Bull. Am. Phys. Soc. **10**, 348 (1965).

[4] R. E. Aldrich, W. J. Burke, and K. A. McCarthy, Solid State Commun. **5**, 899 (1967).

It is helpful to view the curves of Fig. 1 in a direction parallel to the straight section of the pure NaCl curve from 0.3 to 10°K. If one proceeds along any one of the doped thermal-conductivity curves starting from 1°K and working to higher temperatures, then one observes that the separation between the pure and doped curves *increases* uniformly between 2 and 6°K in a way that is very similar to a "resonance dip" in a thermal-conductivity curve that occurs at temperatures above the maximum. Rapid changes in the separation between the impure curve and pure curve at low temperatures are indicative of low-lying excited levels of the impurity. However, in contrast to the higher-temperature resonance dips found in NaCl:AgCl or NaCl:CuCl,[5] where the thermal-conductivity curve of the impure sample recovers to the thermal-conductivity curve of the pure sample below the resonance temperature, the behavior of NaCl:NaOH does not recover below the resonance temperature interval, but again decreases rapidly below 2°K with slopes that are greater than 2.25. In the 0.4–0.8°K range, there is a second resonance dip or "bowl." We assume that for other systems the failure of a doped curve to recover to the pure curve below a resonance region indicates the existence of one or more additional excited levels of the impurity at lower temperatures, as in the case of NaCl:NaOH.

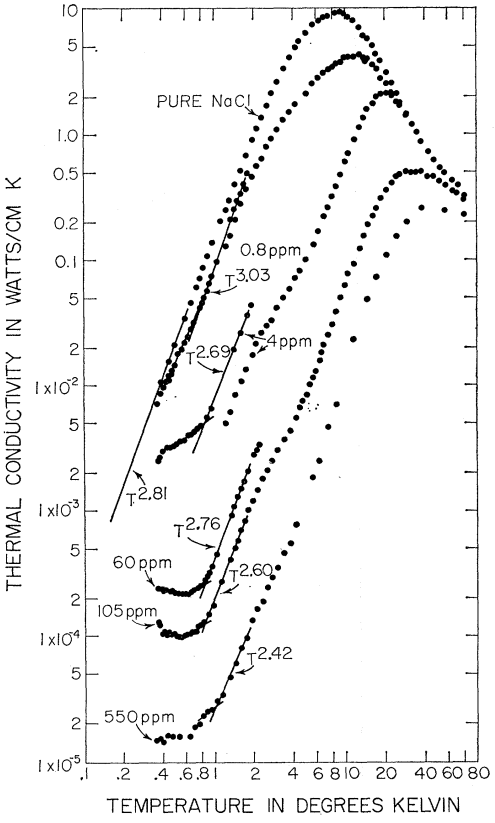


FIG. 1. Thermal conductivity of NaCl:NaOH. The concentrations in parts per million are indicated on the curves. The disconnected parts of the 0.8- and 4-ppm curves were measured at different times.

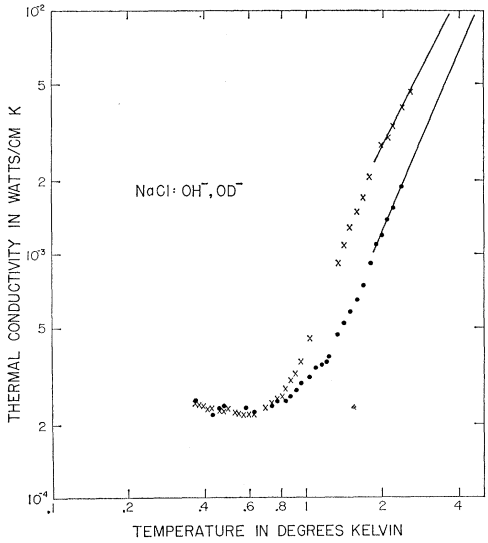


FIG. 2. Thermal conductivity of NaCl with $OH^-$ and $OD^-$. ×, 60-ppm $OH^-$; ●, 50-ppm $OD^-$ (with 19-ppm $OH^-$).

The bowl-shaped region that characterizes the tunneling exhibits some interesting properties. First, there is a very pronounced change in thermal conductivity at 0.86°K indicated by the intersection of pairs of lines for all curves except the 550-ppm curve. For the 550-ppm curve, the break occurs at 1.03°K, perhaps suggesting that dipole-dipole interactions are important in crystals doped higher than 100-ppm hydroxide concentration. The higher dip region between 2–6°K that is well defined in the more lightly doped samples is not well defined in this 500-ppm crystal.

### B. Thermal Conductivity of NaCl:NaOD

The Devonshire model is one particular example from a general group of models which considers the motion about the c.m. of the impurity molecule.[6] Any change in the c.m. reflects a change in the moment of inertia of the molecule and will influence considerably the predictions of the model. The dependence on the moment of inertia may be checked directly by the substitution of deuteroxide $OD^-$ for hydroxide $OH^-$. Any hydrogen tunneling model would predict a smaller value of the energy spacing $\Delta$ between levels and corresponding shifts to lower temperatures in the thermal-conductivity bowl.[6,7] This is not the case as shown in Fig. 2. The negligible differences in the thermal conductivities of $OH^-$ and $OD^-$ in the lower tunneling temperature region strongly suggest that the hydrogen is the pivot site and that the tunneling motion is associated with the oxygen instead. This proposal can be tested by doping

[5] R. F. Caldwell and M. V. Klein, Phys. Rev. **158**, 851 (1967).

[6] A. F. Devonshire, Proc. Roy. Soc. (London) **A153**, 601 (1936).

[7] P. Sauer, Z. Physik **194**, 360 (1966).

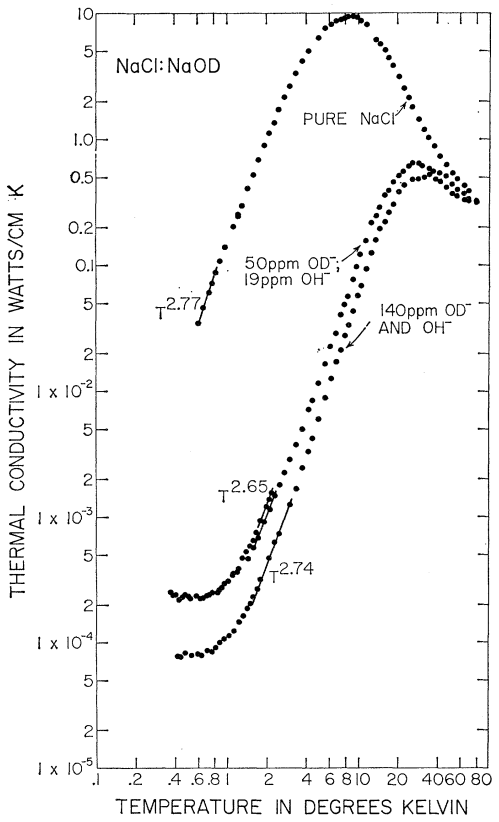


FIG. 3. Thermal conductivity of NaCl:NaOD.

NaCl with enriched $O^{17}H^-$ or $O^{18}H^-$. Figure 3 gives the thermal conductivity of NaCl:NaOD. The thermal-conductivity curves for NaCl:NaOD are very similar in form to the curves of NaCl:NaOH in the 2–10°K region, thus suggesting that the excited levels that occur there are only slightly isotope-dependent.

### C. Calcium in Alkali Halides

The thermal-conductivity measurements on lightly doped NaCl:NaOH were not reproducible from run to run but steadily shifted upward in magnitude with time; the 0.8- and 4-ppm NaCl:NaOH crystals both exhibited the largest discontinuities, where the time lapse between the $He^4$ and more recent $He^3$ measurements was two years. Moreover, small upward shifts in the thermal conductivity have been detected on the 105-ppm NaCl:NaOH upon cycling to room temperature, changing the thermal clamps, and immediately recycling back to 4°K. The time lapse between runs in this case was less than two weeks. Discontinuities also appeared in the following crystals: lightly doped 50-ppm NaCl:NaOD, 36-ppm KCl:KOD, "pure" RbCl and 480-ppm RbCl:RbOH, and the 90-ppm KI:KOH. During this time the thermometers showed no abnormal inconsistencies; hence, we began to suspect that some foreign impurity was acting as a "getter" tying up the hydroxide and destroying its excited states. If indeed the hydroxide ion and divalent impurities such as $Ca^{++}$ were migrating to one another via attractive electrical forces, then the migration taking place at room temperature and during the cyclings to room temperature might be eliminated by quenching the crystal rapidly from 750°C to room temperature; the quenching would produce internal dislocations that would freeze internal migration. Fritz, Lüty, and Anger[8] have suggested that a solid-state chemical reaction takes place at high temperatures between $Ca^{++}$ and 2 $OH^-$ ions yielding $Ca(OH)_2$ or $CaO+H_2O$. Such a reaction could go to completion at 750°C, hence permanently tying up all the $Ca^{++}$ ions in the crystal. We have carried out such an experiment. The thermal conductivity of a freshly grown 60-ppm NaCl:NaOH crystal was first measured, then the crystal was heated to 750°C for 3 h, next quenched from 750°C to room temperature in a couple of minutes, and lastly remeasured two consecutive times without removing the thermal clamps between runs. There was no upward shift between the last two runs which required one week in time—this was our first instance of reproducibility in lightly doped hydroxide crystals. Figure 4 shows the results of the three runs. The last one was not carried out below 1°K.

The starting Mallinckrodt analytical grade NaCl salt, the chlorine treated salt, and the pure crystal grown by the Czochralski method were analyzed for the divalent-ion content. The starting salt as well as the

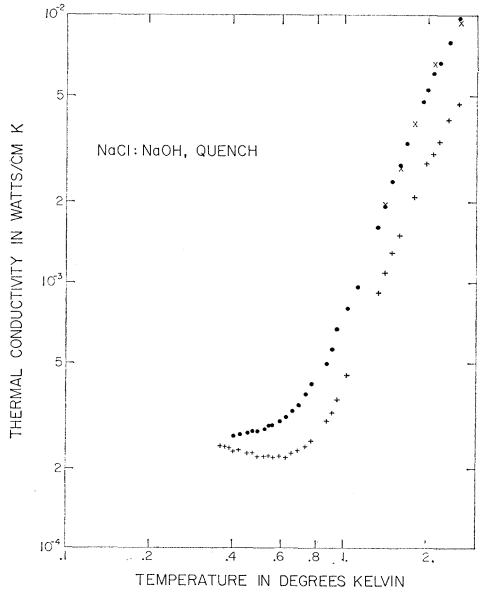


FIG. 4. Effects of quenching a 60-ppm NaCl:NaOH crystal contaminated with calcium. +, the original data on crystal cleaved from boule and sand-blasted prior to measurement; ●, the same crystal after 3-h heat treatment at 750°C followed by a quench to room temperature in 4 min; ×, same crystal measured a third time after completion of the second measurement and warming to room temperature.

[8] B. Fritz, F. Lüty, and J. Anger, Z. Physik **174**, 240 (1963).

chlorine treated salt contained 10–50-ppm divalent ions, primarily $Ca^{++}$. Thus the chlorine treatment removes none of the divalent ions. The Czochralski crystals had 4–20-ppm $Ca^{++}$. Although the detailed study of intentionally doped $Ca^{++}$ crystals with hydroxide is an intriguing and interesting research topic,[8,8a] the large residual calcium background would seem to be harmful to precise thermal-conductivity and specific-heat measurements.[9] For if the divalent impurity is present, not only does the hydroxide ion become immobilized with time, but its excited states are perturbed. Thus it becomes difficult to interpret correctly data on lightly doped hydroxide samples and to study the dipole-dipole interaction. We wish to stress the fact that all crystals mentioned in this paper have modest residual divalent backgrounds of 5–15 ppm, and that no thermal-conductivity measurements have yet been performed by us on crystals grown from ultra-pure starting material.[10]

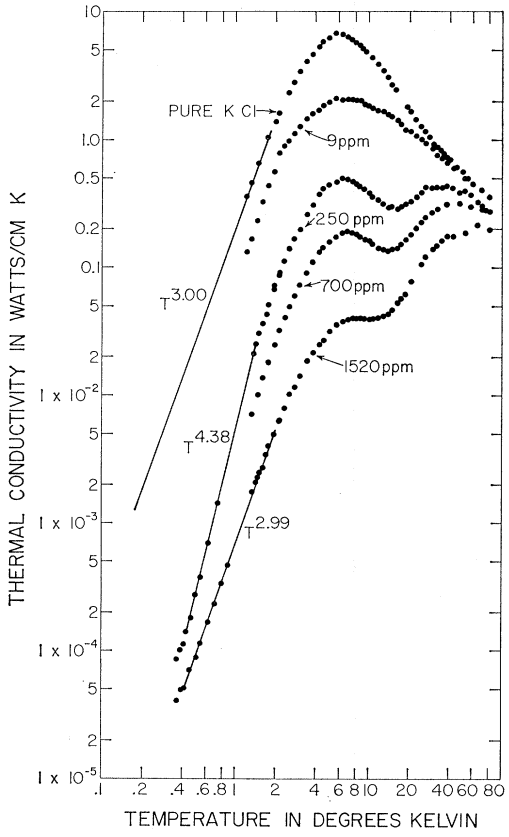


FIG. 5. Thermal conductivity of KCl:KOH. The concentrations in parts per million are indicated on the curves.

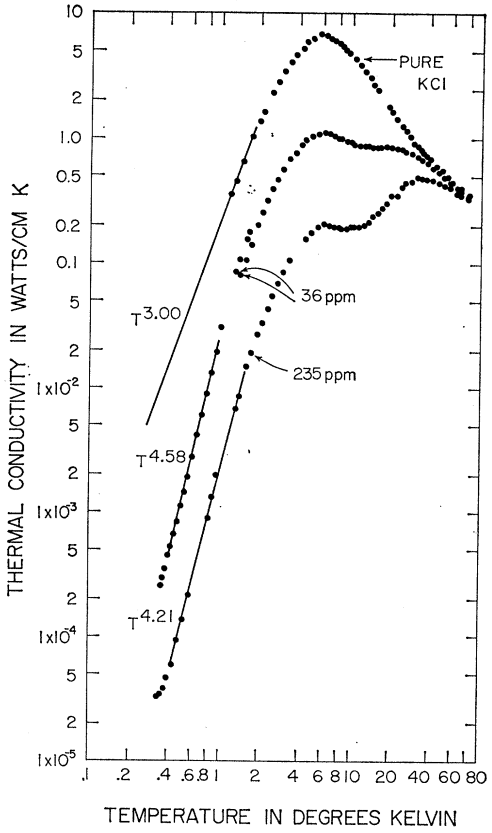


FIG. 6. Thermal conductivity of KCl:KOD. The concentrations in parts per million are indicated on the curves.

### D. Thermal Conductivity of KCl and RbCl

The thermal conductivity of KCl:KOH is similar in many ways to that of NaCl:NaOH. Part of the data has been previously published.[11] The curves in Fig. 5 exhibit a strong dip at 14°K and a depressed conductivity below the conductivity maximum. The depressed conductivity persists down to the lowest temperature measured—0.36°K. Moreover, the very lowest temperature points have a decreased slope, thus suggesting the existence of a bowl-shaped curve and associated tunneling region below 0.3°K.

Near-infrared absorption data on KCl:KOH shows a Lorentzian-type line at 32 $cm^{-1}$ above the first excited vibrational band and a broad shoulder on the high-energy side of the 32 $cm^{-1}$ line.[11,12] The line is strongly temperature-dependent, broadening rapidly between 4.6 and 15°K. In complete contrast to the NaCl:NaOH tunneling lines, the KCl:KOH 32-$cm^{-1}$ line is highly isotope-dependent, shifting down to 23 $cm^{-1}$ with $OD^-$ substitution. This effect is seen dramatically in the KCl:KOD thermal conductivity in Fig. 6.

[8a] A. Kessler, Czech. J. Phys., **B19**, 689 (1969).

[9] J. P. Harrison, P. P. Peressini, and R. O. Pohl, Phys. Rev. **171**, 1037 (1968).

[10] W. J. Fredericks, L. W. Schuerman, and L. G. Lewis, Oregon State University Department of Chemistry reports, 1967 (unpublished).

[11] C. K. Chau, M. V. Klein, and B. M. Wedding, Phys. Rev. Letters **17**, 521 (1966).

[12] B. M. Wedding and M. V. Klein, Phys. Rev. **177**, 1274 (1969).

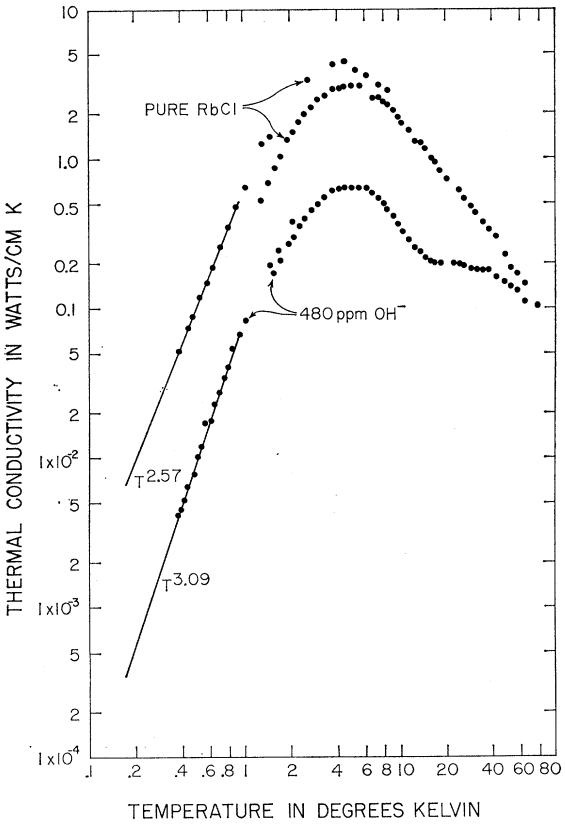


FIG. 7. Thermal conductivity of RbCl:RbOH.

Bosomworth has seen the 32-cm$^{-1}$ line of KCl:KOH directly in the far infrared.[13] This line is strong and somewhat asymmetric above the resonance and has a half-width of 12 cm$^{-1}$ at 1.7°K. It is accompanied by a broad band absorption at higher frequencies. The 32-cm$^{-1}$ line shows no impurity concentration dependence up to 1500-ppm hydroxide concentration. A line[13] at 12 cm$^{-1}$ in NaCl:OH$^-$ may have a similar origin to the 32-cm$^{-1}$ line in KCl:OH$^-$. It is obviously related to our thermal-conductivity dip in the 2–8°K region.

If the trend is established in NaCl:NaOH and KCl:KOH that the heavier host lattice (KCl) has tunneling levels at increasingly lower temperatures and an active far-infrared mode or modes at increasingly higher temperatures, we predict that RbCl:RbOH will have very-low-temperature tunneling levels. Rubidium chloride does have an active infrared mode at 30 cm$^{-1}$ accompanied by a strong and broad absorption that continues up to 100 cm$^{-1}$.[13] The thermal-conductivity data for RbCl:RbOH appearing in Fig. 7 do support the existence of tunneling levels located lower than those of KCl:KOH, since the curve does not at all recover to the pure curve but decreases with a slope of 3.09—one that is larger than the $T^{3.00}$ diffuse boundary scattering. The low-temperature decrease in conductivity per unit hydroxide concentration is much less in RbCl than it is in KCl.

### E. Other Alkali Halides with Hydroxide Impurity

Besides the alkali chloride family, we have superficially probed the iodide and bromide families. The thermal-conductivity curve for KI:KOH in Fig. 8 is especially interesting in that the depressed conductivity indicates the existence of tunneling levels below 0.3°K. These appear to be strong phonon scatterers. The KI:KOH optical data is scant and complicated. Lines have been observed at splittings of 3.7 and 7.5 cm$^{-1}$ above the main vibrational line at 3604 cm$^{-1}$.[12] The 3.7-cm$^{-1}$ line, however, freezes out completely at 1.4°K and is believed to be a side band of the main peak. Wedding and Klein also observed a sharp absorption at a splitting of 13 cm$^{-1}$ (4.88°K).

The alkali bromide thermal-conductivity data are very incomplete, and our interpretation is quite speculative. We show curves for KBr:KOH and NaBr:NaOH in Figs. 9 and 10. The KBr data show a strong dip at 18°K followed by a level plateau that does not rise upward to the thermal conductivity of the pure curve for the highest temperatures. Wedding[12] and Bosom-

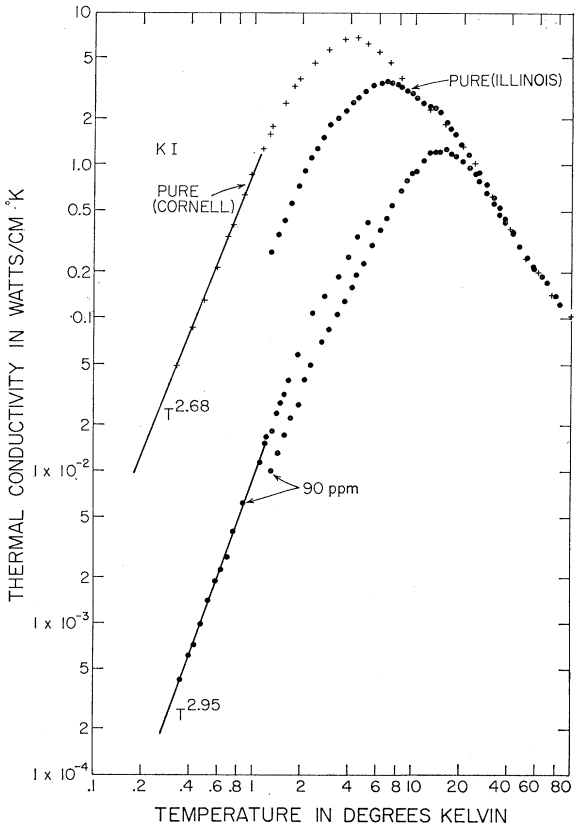


FIG. 8. Thermal conductivity of KI:KOH. The Cornell crystal was measured by Seward and Baumann.

[13] D. R. Bosomworth, Solid State Commun. **5**, 681 (1967).

worth[13] have detected lines at 37.5 $cm^{-1}$ accompanied by very strong absorption up to 90 $cm^{-1}$. Bosomworth has interpreted this strong absorption as an impurity-induced phonon absorption that appears to be similar to the single-phonon-induced absorption found in NaCl:NaAg, NaCl:NaF, and NaCl:NaBr.[14] In addition, Bosomworth has seen a weak isotope shift from 37.5 to 35.0 $cm^{-1}$ upon substitution with $OD^-$.

Another characteristic of the thermal-conductivity data is the depressed nature of the doped curves below the maximum; the thermal conductivity does not approach that of the pure KBr curve. The amount of depression per unit concentration is less than that observed in RbCl, KCl, NaCl, or KI. If this is caused by resonance scattering by tunneling levels, then the cross sections in KBr must be less than those in other lattices, or perhaps the levels are lower in energy. This point will be discussed further at the very end of this paper.

It is possible that the bromide family might exhibit trends similar to those of the chloride family. If so, NaBr:$OH^-$ should have an active far-infrared mode lower than the 37.5-$cm^{-1}$ line in KBr:$OH^-$; also a weak tunneling level should be present in the extreme low-temperature range.

Figure 10 shows NaBr:NaOH thermal-conductivity measurements. The pure Harshaw crystal is believed to contain about 8 ppm $OH^-$. It is interesting that the

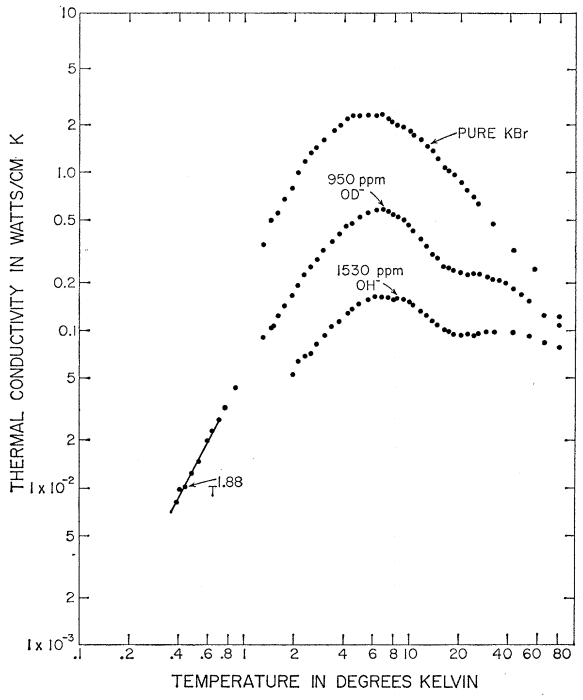


FIG. 9. Thermal conductivity of KBr:KOH and KBr:KOD.

[14] H. F. Macdonald, T. P. Martin, and M. V. Klein, Phys. Rev. 177, 1292 (1969).

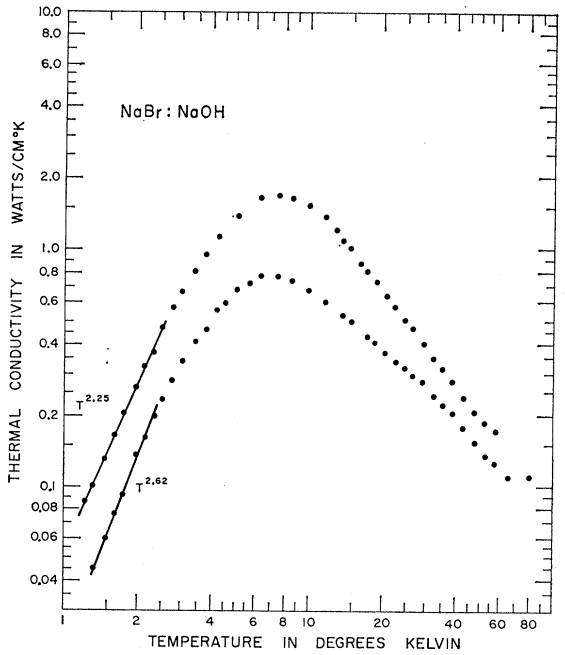


FIG. 10. Thermal conductivity of NaBr:NaOH. The upper curve was taken on a nominally pure Harshaw crystal with 8-ppm $OH^-$. The lower curve on a doped crystal with 64-ppm $OH^-$.

64-ppm NaBr:NaOH curve resembles closely the 9-ppm KCl:KOH curve where a 32-$cm^{-1}$ infrared-active mode is responsible for a 14°K dip. The low-temperature thermal conductivity for the 64-ppm NaBr:NaOH is only weakly depressed but does show a significant slope of 2.62. Higher concentrations of $OH^-$ in NaBr could not be obtained.

## III. ANALYSIS

The present optical and thermal data that are available on the hydroxide ion in any one of the alkali halides have been difficult to interpret in terms of energy-level schemes or microscopic models that give rise to the level schemes. The approach in this paper is to fit the conductivity data through the Debye integral using phenomenological models of the resonances and, wherever possible, to relate model parameters to observed optical data.

Additional insight into good microscopic models will come from experiments yet to be performed, such as the following: (1) half-width dependence of absorption lines upon temperature from microwave and far-infrared measurements, (2) half-width dependence upon hydroxide concentration, (3) growth of hydroxide-doped alkali halide crystals free of divalent ion impurities, (4) the doping of crystals with deuteroxide $OD^-$ that is free of $OH^-$ contamination, (5) thermal-conductivity measurements below 0.4°K, (6) specific-heat measurements from 0.01 to 100°K on samples of wide varying concentrations, (7) Raman scattering, and (8) the study

TABLE I. Values of the parameters used in the Debye thermal-conductivity integral fits to the pure crystals.

| Crystal | Integral constant $k^4/(2\pi^2 v_s \hbar^3)$ W/(cm $K^4$ sec) | $C$ (sec/°K$^n$) | $A$ (sec$^5$) | $B_2$ (sec$^3$/°K$^{G+2}$) | $D$ Dimensionless | $G$ Dimensionless | $n$ Dimensionless |
|---|---|---|---|---|---|---|---|
| NaCl | 3943 | $6.74\times10^5$ | 6.00 | 54 000 | 5.55 | 1.00 | 0.19 |
| KCl | 6561 | $8.41\times10^5$ | 15.00 | 78 000 | 6.76 | 0.95 | 0.00 |

of the electric field and stress-dependent properties of the hydroxide dipole.[15]

### A. Computer Fits to Pure Crystals

The Debye thermal-conductivity integral

$$K(T)=\left(\frac{k^4}{2\pi^2 v_s \hbar^3}\right)\frac{1}{T^2}\int_0^{\theta_D}\tau_c(\nu,T)\frac{\nu^4 e^{\nu/T}}{(e^{\nu/T}-1)^2}d\nu,$$

with $\nu=\omega/k$, $v_s$=sound velocity,

includes within its integrand a combined relaxation time for phonons, $\tau_c(\nu,T)$. The combined relaxation-time term $\tau_c(\nu,T)$ is a transport time or mean time between those phonon collisions which alter the heat current significantly—that is, collisions which change the direction and/or magnitude of the phonon momentum. The combined relaxation time is considered to be a function of the phonon angular frequency $\omega$; it is understood that some sort of average has been taken of a wave-vector-dependent $\tau_c(q)$ over a constant frequency surface. The reciprocal time or combined relaxation rate is assumed to be given by contributions from individual processes by the sum of their individual relaxation rates, $\tau_j^{-1}$:

$$\tau_c^{-1}=\sum_j \tau_j^{-1}.$$

Traditionally, four scattering mechanisms are used to characterize the pure crystal. Once the parameters of these four relaxation rates are adjusted to give the best fit to the thermal conductivity of the pure crystal, an additional relaxation rate is introduced to describe the scattering mechanism of the impurity. The parameters and even the mathematical form of the new relaxation rate will reflect the characteristics of the model assumed for the impurity. The first four relaxation rates for the pure crystal are kept unchanged.

The four relaxation rates for the pure crystal are a boundary rate term, $\tau_b^{-1}=C$, represented by the constant $C$ that is independent of the angular frequency $\omega$ and which yields a $T^3$ temperature dependence to the thermal conductivity at very low temperatures; an isotope term that yields Rayleigh scattering of the form of $A\omega^4$; a "normal" process term $\tau_n^{-1}$ of the form $B_1\nu^2T^G$ in which three phonons interact in such a way to conserve wave vector and hence the heat current; and lastly, an umklapp process term $\tau_U^{-1}$, in the form of $B_2\nu^2T^G e^{-\theta/DT}$ that characterizes phonons interacting with the lattice and, thus, diffuses the heat current. Although the constants $C$, $A$, $B_1$, $B_2$, $D$, and $G$ are related in principle to fundamental constants and properties of the crystal, they are difficult to calculate and often give a poor fit to the data of the pure crystal; for this reason, the constants are treated here as parameters that are not closely related to the theoretical values. The reader is referred to the literature for detailed discussions of the theoretical relaxation rates for a pure crystal.[5,16]

Often the low-temperature thermal conductivity of a pure crystal does not follow a $T^3$ temperature dependence but has a somewhat weaker dependence. For example, our sodium chloride crystals exhibited a $T^{2.81}$ dependence. We attribute this effect to specular reflection at or near the crystal surface. It is assumed that all the NaCl crystals have similar histories and hence exhibit similar boundary scattering mechanisms. Because of this, a weak temperature-dependent factor $T^n$ with small $n$ was incorporated into the boundary constant $C$ to yield the correct temperature dependence of the thermal conductivity at very low temperatures. In the case of KCl, no such factor was used with the constant $C$. In summary, the combined relaxation rate for the pure crystals $\tau_c^{-1}$ takes the form

$$\tau_c^{-1}=\tau_b^{-1}+\tau_{\rm iso}^{-1}+\tau_n^{-1}+\tau_u^{-1}.$$

The actual expression used was

$$\tau_c^{-1}=CT^n+A\nu^4+B_2\nu^2T^Ge^{-\theta/DT}.$$

A separate normal-process contribution was not used. The values of the parameters for the pure crystal fits appear in Table I.

### B. Some Predictions of a General Theory of Resonances

From the thermal-conductivity data on hydroxide in NaCl, there appears to be one or more excited levels of hydroxide below 1°K; far-infrared data show that there are at least five levels above 1°K. Presumably, phonons interact strongly with the hydroxide ion, virtually

[15] In this last area much is already known. See F. Lüty, J. Phys. (Paris) 28, Suppl. C-4, 120 (1967).

[16] C. T. Walker and R. O. Pohl, Phys. Rev. 131, 1433 (1963); J. W. Schwartz and C. T. Walker, *ibid.* 155, 959 (1967); W. D. Seward and V. Narayanamurti, *ibid.* 148, 463 (1966); V. Narayanamurti, W. D. Seward, and R. O. Pohl, *ibid.* 148, 481 (1966); L. G. Radosevich and C. T. Walker, *ibid.* 171, 1004 (1968); F. C. Baumann, J. P. Harrison, R. O. Pohl, and W. D. Seward, *ibid.* 159, 691 (1967).

exciting it to a higher energy state in a type of resonance interaction. A multiple-level tunneling system will have much in common with a simple two-level tunneling system or with a harmonic-oscillator resonance. In a recent paper, resonant-phonon scattering from a two-level tunneling system has been discussed and compared with that from a substitutional impurity with an internal harmonic-oscillator degree of freedom and with that from a simple substitutional impurity atom.[17] The results for the average impurity-induced resonance scattering rate for all phonons of frequency $\omega$ could be written in a common form. For a crystal with two atoms per unit cell, the result in the Lorentzian approximation is

$$\langle\tau_i^{-1}\rangle(\omega,T)=\frac{pd}{3\pi\rho(\omega_r)}\frac{\Gamma(0)\Gamma(T)S(T)}{(\omega^2-\omega_r^2)^2+\Gamma(T)^2}. \quad (1)$$

Here $p$ is the fractional impurity concentration, $d$ the degeneracy of the resonance mode (3 for an infrared-active $T_{1u}$ mode),[18] $\rho(\omega)$ the total (unperturbed) phonon density of states normalized to unity, $\omega_r$ the resonance angular frequency, $\Gamma(T)$ the (possibly) temperature-dependent half-width of the resonance at half-maximum when considered as a function of $\omega^2$, and $S(T)$ is the temperature-dependent strength of the resonance.

In obtaining Eq. (1), an assumption was made that a single "configuration" or linear combination of lattice displacements is coupled bilinearly to the resonance. The zero-temperature width $\Gamma(0)$ is then proportional to a coupling constant times $\mathrm{Im}G(\omega_r)$, the imaginary part of the phonon Green's-function diagonal in this configuration. Some comments about the use of a frequency-averaged scattering rate will be made at the end of this paper.

For a harmonic-oscillator impurity or a simple substitutional impurity atom, in a harmonic lattice, there is no temperature dependence to $\Gamma(T)$, and $S(T)$ is identically unity. For a two-level tunneling system with no other coupling or decay mechanisms, the temperature-dependent strength factor is

$$S(T)=\tanh\tfrac{1}{2}\beta\hbar\omega_r, \quad (2)$$

with

$$\beta=(kT)^{-1}.$$

Equation (2) results from a correct treatment of the occupation probabilities for the ground and excited tunneling states. The decay of the excited state is by a direct one-phonon mechanism and hence

$$\Gamma(T)=\Gamma(0)\coth(\theta/2T), \quad (3)$$

with

$$\theta=\hbar\omega_r/k.$$

Because of anharmonic or other neglected effects, $\Gamma(T)$ and $S(T)$ may be different from Eqs. (2) and (3). An impurity with an internal *an*harmonic oscillator degree of freedom may also have different expressions for $\Gamma(T)$ and $S(T)$.

For additional discussions of linewidths of tunneling systems, see the papers of Vredevoe,[19] Dick,[20] and Fong.[21] Vredevoe and Dick consider life-time broadening; Fong considers broadening due to interactions with strains and other $OH^-$ ions.

Important contributions of $\tau_i$ to the thermal-conductivity integral are made away from resonance. Then the shape of the wings of the resonance curve is important, and it is necessary to use a frequency-dependent width. This can be done by letting $\Gamma$ be proportional to (coupling constant)$\times\mathrm{Im}g(\omega)$ instead of to (coupling constant)$\times\mathrm{Im}g(\omega_r)$ and by using $\rho(\omega)$ instead of $\rho(\omega_r)$ in Eq. (1). For the usual case of low-frequency resonances, we require the limiting dependence in the low-frequency limit. Then $\rho(\omega)=(\omega/\omega_r)^2\rho(\omega_r)$. The frequency dependence of $\Gamma$ for many cases has already been discussed.[22–24] For a substitutional mass defect $\mathrm{Im}g\sim\omega$, but the coupling constant is $(-\Delta M/M)\omega^2$, so that $\Gamma\sim\omega^3$. We can write this in the form

$$\Gamma(\omega)=(\omega/\omega_r)^3\Gamma(\omega_r)=\omega_r^2(\omega/\omega_r)^3\gamma. \quad (4)$$

Here $\gamma=\Gamma(\omega_r)/\omega_r^2$ is the dimensionless width at $\omega=\omega_r$. The same expression results for a resonance in a breathing or similar even-parity configuration or for a harmonic-oscillator impurity coupled to such a configuration, for then the coupling constant is a force constant and is frequency-independent, but $\mathrm{Im}g\sim\omega^3$. For an odd-parity $T_{1u}$ pure force-constant resonance or for coupling of a harmonic oscillator to such a configuration, $\mathrm{Im}g\sim\omega^5$ and

$$\Gamma(\omega)=\omega_r^2(\omega/\omega_r)^5\gamma. \quad (5)$$

We write Eqs. (4) and (5) in the form

$$\Gamma(\omega)=\omega_r^2(\omega/\omega_r)^{n+1}\gamma, \quad \text{with } n=2, 4. \quad (6)$$

For a two-level tunneling resonance coupling to the above mentioned configurations, the values of $n$ in Eq. (6) must be increased by 1.[25]

[17] M. V. Klein, preceding paper, Phys. Rev. **186**, 839 (1969).

[18] The insertion of a factor $d$ is justified for a substitutional impurity atom or harmonic oscillator. For a two-level tunneling system $d=1$. A tunneling system in which one or more of the levels is degenerate was not treated in Ref. **17**. For an example of such a system treated by perturbation theory, see A. Griffin and P. Carruthers, Phys. Rev. **131**, 1976 (1963). It is not yet clear whether certain hydroxide levels are more like harmonic-oscillator levels or like tunneling levels. An example is the 32-$cm^{-1}$ level in KCl:$OH^-$ (Fig. 11). If it is an oscillator, it is probably twofold degenerate (Ref. 12).

[19] L. A. Vredevoe, Phys. Rev. **153**, 312 (1967).

[20] B. G. Dick, Phys. Status Solidi **29**, 587 (1968).

[21] C. Y. Fong, Phys. Rev. **165**, 462 (1968).

[22] M. V. Klein, Phys. Rev. **131**, 1500 (1963); **141**, 716 (1966).

[23] J. A. Krumhansl, in *Proceedings of the International Conference on Lattice Dynamics, Copenhagen, Denmark, 1963*, edited by R. F. Wallis (Pergamon Press, Ltd., Oxford, England, 1964), p. 523.

[24] M. V. Klein, in *Physics of Color Centers*, edited by W. B Fowler (Academic Press Inc., New York, 1968) Chap. 7.

[25] Reference 17, Eq. (4-29).

The generalization of Eq. (1) for a frequency-dependent width is then

$$\langle\tau_i^{-1}\rangle=\frac{pdS(T)}{3\pi\rho(\omega_r)}\frac{\gamma(T)\gamma(0)(\omega/\omega_r)^{2n}}{(1-\omega^2/\omega_r^2)^2+\gamma(T)^2(\omega/\omega_r)^{2n+2}}. \quad (7)$$

Note that if Eqs. (2) and (3) are valid, there is no temperature dependence in the product $S(T)\gamma(T)$.

For a multilevel tunneling system, there has been no calculation as general as that leading to Eq. (7). One might try an *ad hoc* superposition of terms of the form of Eq. (7), one for each transition. The product $dS(T)$ would then take into account the degeneracies and the difference in occupation probabilities for the two levels involved in a given transition. $\gamma$ would be the sum of the widths of the two levels, which might vary considerably among levels because of varying selection rules and couplings to phonons of different symmetry.

### C. Calculated Conductivity Curves

We now present the results of a partial application of Eq. (7) to our conductivity data on KCl:$OH^-$ and NaCl:$OH^-$. The application is incomplete because the curves to be shown here were calculated before the full theory in Ref. 17 and Eq. (7) was developed. The most important feature of Eq. (7) that we did not realize at the time was that it contains no adjustable parameters apart from $d$, $\gamma(0)$, $\gamma(T)$, and $S(T)$; our earlier phenomenological result was

$$\langle\tau^{-1}\rangle=\frac{Cp\gamma(T)(\omega/\omega_r)^{2n}}{(1-\omega^2/\omega_r^2)^2+\gamma(T)^2(\omega/\omega_r)^{2n+2}}, \quad (8)$$

where $C$ was an unknown constant having the dimensions of a frequency. Fits were originally tried with adjustable temperature-independent $\gamma$'s and adjustable values of $C$. The shapes of the curves would have been in better agreement if a temperature-dependent $\gamma(T)$ was used; this was necessary to obtain the right kind of dip or depression. A stronger $T$ dependence than that of Eq. (3) was tried, namely,

$$\gamma(T)=\gamma(0)\coth(\theta'/2T), \quad \text{with } \theta'\approx\hbar\omega_r/(4k). \quad (9)$$

This worked well, and other expressions were not tried. This is unfortunate, since we do not really know how sensitive our calculated curves are to the temperature dependence of $\gamma(T)$. We do feel, however, that Eq. (9) works better than no temperature dependence at all. This point should be investigated in much more detail.

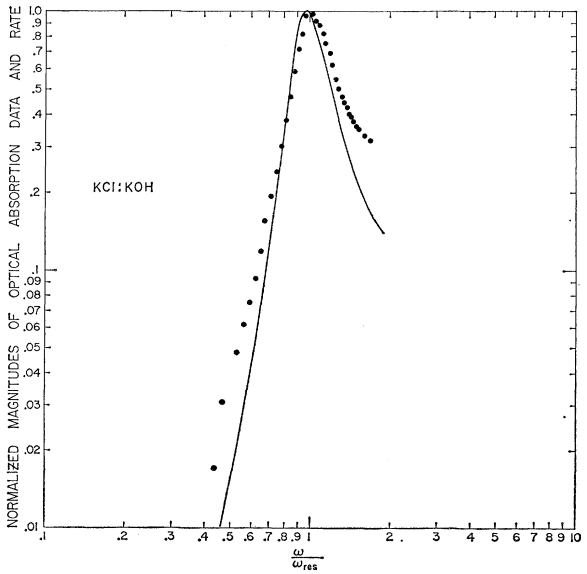


FIG. 11. The fitting of Eq. (7) or (8) (black line) to the low-temperature far-infrared data of Ref. 13 (solid dots).

### *KCl*

Several attempts were made to fit the experimental data on KCl:KOH. For the high-temperature dip the experimental far infrared value of 32 $cm^{-1}$ or $60.3\times10^{11}$ rad/sec was used and calculations were made with $n=2$ and $n=4$. The latter value produced curves that had the dip in the wrong place; this could be corrected by using $\frac{1}{2}\omega_r$ instead of $\omega_r$ in Eq. (8). This can be understood as follows. With a relatively large value of $\gamma(T)$ (see below), the peak in $1/\tau_i$ will be shifted upwards from $\omega_r$ because of the steeply rising $\omega^{2n}$ factor in the numerator. The quantitative agreement between the values of $C$ needed for the fit and the prediction of Eq. (7) was way off when $n=4$ was used. We, therefore, feel that the configuration to which the resonance is coupled does indeed have an Img proportional to $\omega^3$ and that this should be an important feature of any microscopic model of $OH^-$ in KCl.

It is shown in Ref. 17 that for Img$\sim\omega^3$, $\tau_i^{-1}(\omega)$ should be directly proportional to the impurity-induced infrared absorption constant in the vicinity of the resonance. The fitting of Eq. (7) or (8) with $n=2$ to the low-temperature far-infrared data[13] is shown in Fig. 11. The low-$T$ value of $\gamma$ was 0.375. At finite temperatures we used Eq. (9) with $\theta'=12°$, such that

$$\gamma(T)=0.375\coth(12/2T),$$

and calculated the conductivity curves shown in Fig. 12. The low-temperature region will be discussed shortly. The curves shown were calculated using Eq. (7) with the following values of $C$ (in units of $10^{13}$ rad/sec): $C=8.8$ at $p=9$ ppm, $C=3.2$ at 250 ppm, $C=3.9$ at 700 ppm, and $C=1.8$ at 1520 ppm. A comparison of Eq. (8) with Eq. (7) for $S(T)=1$ gives the prediction

$$C=\gamma(0)d/3\pi\rho(\omega_r). \quad (10)$$

We estimate $\rho(\omega)\approx0.75\times10^{-40}\omega^2$ (sec) for KCl on the basis of a small increase over the computed value $\rho=0.5\times10^{-40}\omega^2$ for NaCl.[5] Then using $d=2$, which would apply to a torsional mode perpendicular to the O-H axis, as suggested by infrared dichroism measure-

ments,[12,20] we find

$$C=2.9\times10^{13}\ \text{rad/sec}.$$

This good quantitative agreement with the "experimental" values of $C$ quoted above is uncertain to the extent that the proper temperature dependence of $\gamma$ is uncertain. The conductivity dip occurs at 14°K, and $\gamma(14°)/\gamma(0)=2.5$. Thus, the calculated values of $1/\tau$ may be off by as much as this factor. But we do feel that the infrared width used with Eq. (7) does give the calculated conductivity curves within a factor of 2–3 of the measured curves.

The low-temperature fits in Fig. 12 are not very precise because measurements did not extend into the true dip region. Nevertheless, it is possible to get an estimate of a characteristic linewidth of the low-lying tunneling levels. We rather arbitrarily selected two resonance frequencies at 0.47 and 0.86 cm$^{-1}$. The values for $\theta$ in Eq. (9) were 0.14° in both cases. The ratios of the $C$ values were the same as those stated above for the 32-cm$^{-1}$ resonance. $\gamma$ was treated as an unknown. The strength factor $S(T)$ was assumed to be unity. The values of the product $B=C\gamma$ used for the 700-ppm curve were $0.8\times10^{11}$ and $1.3\times10^{11}$ rad/sec. Neglecting any $T$ dependence of $\gamma$ and assuming a degeneracy $d=3$, one finds that $B$ should be given by $\gamma^2/\pi\rho(\omega_r)$. This would predict a value of $0.9\times10^{-3}$ for the $\gamma$ value for the 0.86-cm$^{-1}$ level, corresponding to a linewidth $\Delta f$ of about $1.5\times10^{8}$ Hz or to a lifetime $\tau=(\Delta f)^{-1}\sim0.6\times10^{-8}$ sec.

*NaCl*

The NaCl data were fitted using a superposition of seven resonance terms having the general form of Eq. (8) with $n=2$:

$$\langle\tau_i^{-1}\rangle=rp\sum_{j=1}^{7}\frac{C_j\gamma_j(T,p)(\omega/\omega_j)^4S_j(T)}{(1-\omega^2/\omega_j^2)^2+[\gamma_j(T,p)]^2(\omega/\omega_j)^6}. \quad (11)$$

In order to keep the low-temperature break at a constant 0.9°K, as given by the experimental data, we found it necessary to use temperature- and concentration-dependent widths $\gamma_j(T,p)$. In addition, an over-all concentration-dependent strength factor $r$ was used in Eq. (11). The values of $r$ are given in Table II. The low value for $r$ at $p=0.8$ ppm probably means that most of the hydroxyl ions in the crystal were not contributing to the phonon scattering—probably because they were tied up by impurities. The dominant effect of $\gamma_j(T,p)$ is in the numerator of each term in Eq. (11), and the necessity for the factor $r$ outside the integral may imply that we did not use a strong enough concentration dependence for $\gamma_j$. The expression actually used was

$$\gamma_j(T,p)=\gamma_j(0)(1+2000\,rp)\coth(\theta_j/2T). \quad (12)$$

An independent justification for use of a concentration dependent $\gamma_j$ is found in the experimental far-infrared absorption data. Bosomworth's line or lines at $p=1900$ ppm[13] are much broader than the lines observed by Kirby *et al.* in NaCl:OH$^-$ at 60 ppm.[26] The values of $\gamma_j(0)$ used for the fits to the conductivity curves are given in Table III. They were chosen to be consistent with the data of Kirby *et al.*, but no attempt was made to resolve their curve into individual lines and to determine individual widths.

The transitions used in Table III can be related to the energy-level diagram shown in Fig. 13. This scheme is somewhat arbitrary and it certainly is incomplete (for example, the weak 10.3-cm$^{-1}$ level of Kirby *et al.* is not shown), but we believe it has some validity. Transitions

TABLE II. Relative strengths used to fit NaCl:OH$^-$ conductivity curves.

| Hydroxide concentration $p$ (ppm) | Relative strength $r$ |
|---|---|
| 0.8 | 0.05 |
| 4 | 0.77 |
| 60 | 0.52 |
| 105 | 1.00 |
| 550 | 1.4 |

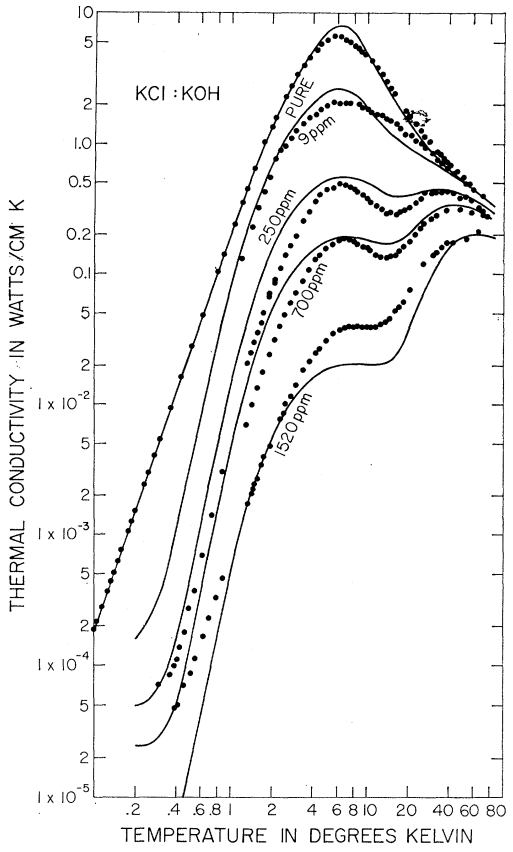


FIG. 12. Thermal conductivity of KCl:KOH. The dots represent experimental data for the concentrations indicated in parts per million. The solid lines represent computed curves.

[26] R. D. Kirby, A. E. Hughes, and A. J. Sievers, Phys. Letters **28A**, 170 (1968).

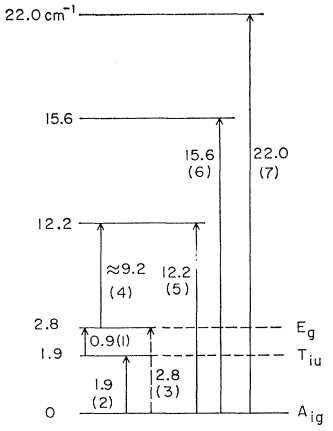


FIG. 13. Partial energy-level scheme for NaCl:NaOH. The numbers in parenthesis refer to the number ($j$) of the transition in Table III.

at 9.2, 12.2, 15.6, and 22.0 cm$^{-1}$ have been seen by Kirby *et al.* in the far infrared. They also observed a strong 2-cm$^{-1}$ transition. As shall be shown, the low-temperature dip in our NaCl:OH$^-$ conductivity data implies a transition at about 1 cm$^{-1}$ that does not involve the ground state. This feature combines with the 2-cm$^{-1}$ far-infrared level to suggest a simple three-level system for the lowest multiplet of the $A_{1g}$, $T_{1u}$, $E_g$ tunneling type.[27,28]

The temperature-dependent strength factors $S_j(T)$ used in Eq. (11) are listed in Table III. The probabilities $P(A_{1g})$, etc. are those for occupation of a single one of the three lowest levels and are assumed to be

$$P(A_{1g})=1/D,\ P(T_{1u})=e^{-2x}/D,\ P(E_g)=e^{-3x}/D, \quad (13)$$

with $D=1+3e^{-2x}+2e^{-3x}$ and $x=0.35°/T$ (corresponding to the 0.92-cm$^{-1}$ transition). These expressions represent an approximation since thermal occupation of the upper level in any of the seven transitions has been neglected. One could argue, for instance, that the strength of an $A_{1g}\rightarrow T_{1u}$ transition should go to zero at high temperatures and be proportional to $(1-e^{-2x})/D$. It is not clear how to account for these effects without knowing more details about the correct energy levels such as degeneracies. We have therefore neglected them, but we have kept what we believe is the main feature necessary for a good fit, namely a temperature-dependent strength for the lowest or 0.9-cm$^{-1}$ transition that decreases to zero at low temperatures. $P(T_{1u})$ has this property. Curve a in Fig. 14 represents our fit using Eqs. (11)–(13) and Tables II and III. When $P(T_{1u})$ is replaced by unity for the $j=1$ transition, curve d is obtained. A strong minimum at 0.6°K is obtained only by allowing for a low-temperature freezing out of this

TABLE III. Parameters of transitions used to fit conductivity data on NaCl:OH$^-$ (105 ppm).

| Transition ($j$) | $\omega_j$ ($10^{11}$ rad/sec) | $\omega_j$ (cm$^{-1}$) | $S_j(T)$ | $\theta_j$ (deg K) | $\gamma_j(0)$ | $\gamma_{tj}^2$ |
|---|---|---|---|---|---|---|
| 1. $T_{1u}\rightarrow E_g$ | 1.7 | 0.9 | $P(T_{1u})$ | 0.55 | 0.10 | $0.5\times10^{-4}$ |
| 2. $A_{1g}\rightarrow T_{1u}$ | 3.5 | 1.9 | $P(A_{1g})$ | 0.55 | 0.10 | $1.0\times10^{-4}$ |
| 3. $A_{1g}\rightarrow E_g$ | 5.2 | 2.8 | $P(A_{1g})$ | 0.83 | 0.10 | $0.92\times10^{-4}$ |
| 4. $E_g\rightarrow 12$ cm$^{-1}$ | 17.4 | 9.2 | $P(E_g)$ | 2.75 | 0.10 | $2.55\times10^{-3}$ |
| 5. $A_{1g}\rightarrow 12$ cm$^{-1}$ | 23.0 | 12.2 | 1 | 3.6 | 0.15 | $1.35\times10^{-3}$ |
| 6. $A_{1g}\rightarrow 15$ cm$^{-1}$ | 29.4 | 15.6 | 1 | 4.7 | 0.10 | $1.1\times10^{-3}$ |
| 7. $A_{1g}\rightarrow 22$ cm$^{-1}$ | 41.4 | 22.0 | 1 | 6.5 | 0.14 | $2.0\times10^{-3}$ |

$j=1$ transition. This fact provides good evidence that the lowest energy transition does not involve the ground state. This qualitative conclusion is probably valid even if the quantitative forms assume for the energy levels and for $S_j(T)$ are not correct.

The use of $x=0.35°/T$ in Eq. (13) is consistent with the small values of $\theta_j$ used in Eq. (12), but not with the interpretation of $P(A_{1g})$, $P(T_{1u})$, and $P(E_g)$ as occupation probabilities for the lowest three levels in Fig. 13. Additional machine calculations have shown that con-

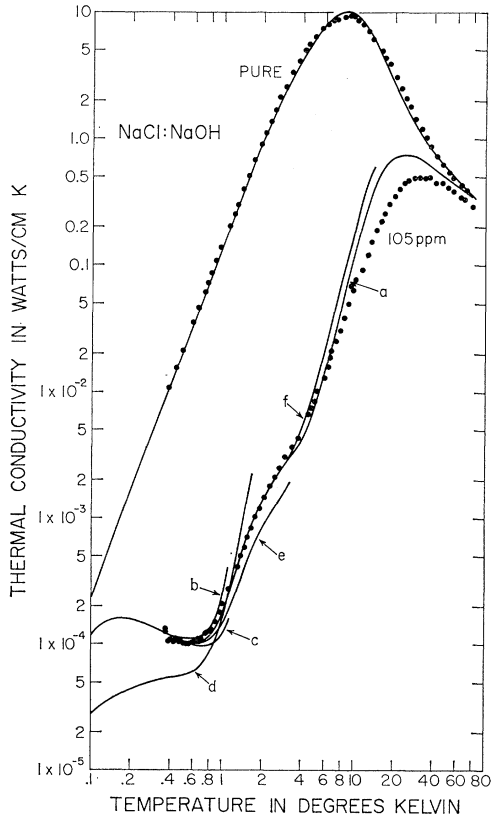


FIG. 14. Computer fits to the thermal conductivity of the 105-ppm NaCl:NaOH crystal. The dots represent the experimental data; the solid lines are calculated curves. Curve a: All the transitions in Table III. Curve b: transition (3) excluded. Curve c: transition (3) included with greater strength than in Table III. Curve d: $P(T_{1u})$ for transition (1) replaced by unity. Curve e: $P(E_g)$ for transition (4) replaced by unity. Curve f: no 15.6- and 22.0-cm$^{-1}$ transitions included (transitions 6 and 7).

[27] G. Feher, I. W. Shepherd, and H. B. Shore, Phys. Rev. Letters **16**, 500 (1966).

[28] H. B. Shore, Phys. Rev. **151**, 570 (1966); M. E. Baur and and W. R. Salzman, *ibid.* **151**, 710 (1966); T. L. Estle, *ibid.* **176**, 1056 (1968).

sistency can be restored by lowering the splittings of the first three levels by about 40%; $\omega_1$ and $\omega_2$ then agree fairly well with observed microwave thransitions at 0.6 and 0.9 $cm^{-1}$ found by Scott and Flygare.[29] With $x$ in Eq. (13) given by $\hbar\omega_1/k$, these adjusted frequencies give curves close to those in Fig. 14.

There is good optical evidence that the 9.2-$cm^{-1}$ $j=4$ transition freezes out for $T\lesssim 4°K$.[12,26] When we replace the factor $P(E_g)$ used for the fourth transition by unity, we obtain curve e instead of curve a. The change is not as dramatic as with curve d, but it does suggest that a transition near 9 $cm^{-1}$ is important for the conductivity and that it freezes out at low temperatures.

The $j=3$ transition, if it were indeed an $A_{1g}\rightarrow E_g$ transition, would be infrared-inactive. It would be "phonon-active," however; if it is omitted, curve b is obtained. If its strength is increased over that in Table III, curve c is obtained.

The high-temperature fit in Fig. 14 is less successful than that at low temperatures, perhaps, because we did not include enough high-energy transitions or perhaps we underestimated the widths or strengths of such transitions relative to those of lower frequency. When the 15.6- and 22.0-$cm^{-1}$ transitions are excluded, curve f is obtained.

The values of $\gamma_j(0)$ used are rough estimates of the true widths, which we shall denote by $\gamma_{jt}$. Since the main effect of $\gamma$ is in the numerator, we can compare the product $c_j\gamma_j(0)$ with the predictions of Eq. (7). If we neglect possible difficulties with temperature-dependent $\gamma$'s and $S$'s and assume a degeneracy $d=2$, we would predict

$$\gamma_{jt}^2=\tfrac{1}{2}3\pi\gamma_j(0)C_j\rho(\omega_j). \qquad (14)$$

Numerical values for the right-hand side of Eq. (14) are given in the last column in Table III. These results predict widths $\gamma_{jt}\sim 10^{-2}$ for the lower set of levels, i.e., tunneling levels, about one order of magnitude greater than our estimate for tunneling widths in $KCl:OH^-$. The higher levels in NaCl would have $\gamma_{jt}\sim 1/30$, which is smaller than the experiments of Kirby *et al.*[26] The full fits are shown in Fig. 15.

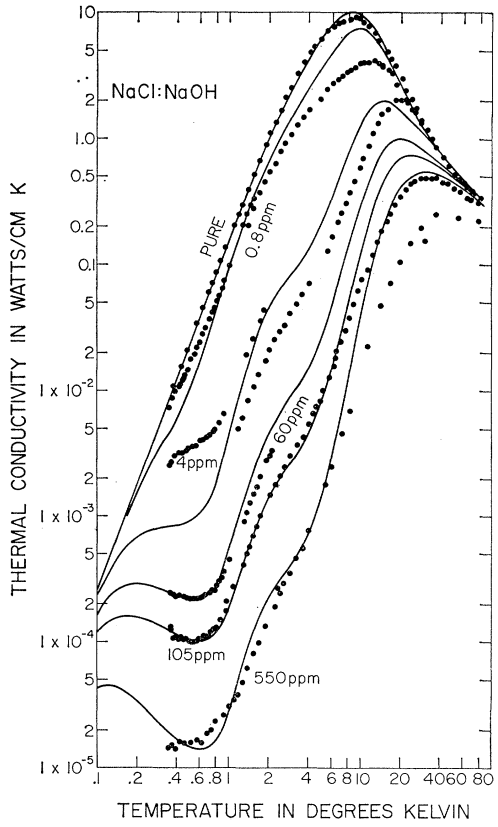


FIG. 15. Thermal conductivity of NaCl:NaOH. The dots represent experimental data. The solid lines represent theoretical calculations using the parameters of Tables II and III. The hydroxyl concentrations are indicated in parts per million.

## IV. CONCLUDING DISCUSSION

In this work simple Lorentzians were not used to fit the conductivity data. Instead allowance was made for the frequency dependence of the imaginary part of the resonance denominator. The result is a strong frequency dependence in the numerator of the expression for the average scattering rate $\langle\tau^{-1}\rangle(\omega)$, which can change the shape of the calculated resonance dip and the temperature at which it occurs. In the case of an isolated infrared resonance, such as the one at 32 $cm^{-1}$ in $KCl:OH^-$, this fact may be used to determine $n$ in Eq. (7). The data suggest that $n=3$ for this resonance in KCl and probably also for many resonances in NaCl. This will have to be explained by a microscopic theory of the energy levels and their coupling to phonons. With octahedral symmetry, this value of $n$ is characteristic of even-parity phonon modes, such as breathing modes.[22–24] These could not couple to infrared-active internal or external modes of the impurity. Because of the low symmetry of the hydroxyl ion, we believe that for at least many of the energy levels the effective site symmetry is lower than octahedral with parity no longer a good quantum number, and it is then possible for infrared-active modes to couple to certain modes of nominal even parity.

In sodium chloride there were definite concentration-dependent effects, mainly in the form of concentration-dependent widths, although concentration-dependent strengths cannot yet be ruled out. This lattice provided a deep low-temperature conductivity dip that could be understood only by assuming that the lowest-energy transition did not involve the ground state. This is an important new result. This lowest temperature dip did not shift when $OD^-$ was substituted for $OH^-$; tunneling of the hydrogen part of the hydroxyl ion does not seem to be responsible for the lowest set of tunneling levels.

The reason for averaging $1/\tau$ over a constant frequency surface is, firstly, that it leads to a simple result

[29] R. S. Scott and W. H. Flygare, Phys. Rev. **182**, 445 (1969).

and, secondly, that it seems to work. But why should all phonons of a given frequency have the same scattering rate? The resonance levels are not likely to couple to all phonons of the same frequency with equal strength. Those coupled weakly or not coupled at all would tend to provide a "short-circuit" for the heat current. This evidently does not happen to any significant extent. A probable reason is that there is enough anharmonicity present to couple these phonons that do not "see" the resonance with those that do see it via multiple-phonon interactions. These higher order processes would have to occur at the impurity so that they can keep pace with the resonance scattering at high concentrations, as required by our data; otherwise, the cross section would decrease at higher concentrations.

This anharmonic mixing must be very efficient for the 32-$cm^{-1}$ level in KCl:$OH^-$ to account for our successful fit to the data. The data are not very good for the tunneling levels in KCl, because we did not go low enough in temperature, but our estimate of a lifetime of $0.6\times10^{-8}$ sec is consistent with experimental values of reorientation times of $1\times10^{-8}$ sec determined in optical and dielectric measurements.[15,30] The experimental widths of electric resonance lines in KCl:$OH^-$ are much broader than this $10^{-8}$-sec lifetime would predict.[27,31] They are undoubtedly inhomogeneously broadened due to interactions with strains and other hydroxyl ions.[21] This will produce a continuous distribution $f(\omega_r)$ of resonance frequencies. The right side of Eq. (7) may be regarded as giving $\langle\tau_i^{-1}\rangle_{\omega r}$ for a single resonance at $\omega=\omega_r$. The inhomogeneous scattering rate would be

$$\langle\tau_i^{-1}\rangle_{\text{inh}}=\int f(\omega_r)\langle\tau_i^{-1}\rangle_{\omega r}d\omega_r.$$

This will be smaller than the expression obtained from Eq. (7) alone with $\gamma(T)$ replaced by the inhomogeneous linewidth.

For NaCl:$OH^-$ our values of $\gamma$ are less than one would predict from the far-infrared data.[26] This is particularly true for the 2-$cm^{-1}$ transition ($j=2$ in Table II), for which the data of Kirby *et al.* gives $\gamma\approx1$, whereas we have estimated $\gamma\sim10^{-2}$. The corresponding lifetime from our data is then about $0.3\times10^{-10}$ sec, roughly one-thirtieth of that estimated from the reorientation data provided by Lüty.[15] If we assume that Lüty's results and ours are in crude agreement with each other, the implication is that, like the electric resonance lines, the far-infrared lines are inhomogeneously broadened at 60 ppm, as we know they are at 1900 ppm.[13] From the fact that we found it necessary to use a concentration-dependent width in NaCl and from the fact that our width is 30 times that of Lüty, one can tentatively conclude that inhomogeneous broadening of resonance lines does increase the phonon-scattering rate, but not as much as homogeneous broadening would. This is a topic for more detailed future investigation.

In decreasing order, the effectiveness of the hydroxyl ion as a low-temperature phonon scatterer is as follows: NaCl, KI, KCl, RbCl, and KBr. Except for the order of NaCl and KI, this is precisely the order of increasing lifetimes for $OH^-$ reorientation.[15,20] This supports the thrust of our argument that strong low-temperature conductivity depressions can be caused by low-frequency resonances only if the lifetime-determined width is relatively large.

## ACKNOWLEDGMENTS

We are very grateful to Martin Ferer for his assistance on the computer calculations. We are also indebted to Roger D. Kirby for much correspondence concerning his data.

[30] U. Bosshard, R. W. Dreyfus, and W. Känzig, Physik Kondensierten Materie **4**, 254 (1965).

[31] W. E. Bron and R. W. Dreyfus, Phys. Rev. Letters **165**, (1966); Phys. Rev. **163**, 304 (1967).